DEVELOPMENT OF WAKE VORTICES AND THE ASSOCIATED SOUND RADIATION IN THE FLOW PAST A RECTANGULAR CYLINDER OF VARIOUS ASPECT RATIOS

Ayumu INASAWA
Department of Aerospace Engineering
Tokyo Metropolitan University
6-6 Asahigaoka, Hino, Tokyo 191-0065, JAPAN
ainasawa@sd.tmu.ac.jp

Takuya NAKANO
Department of Aerospace Engineering
Tokyo Metropolitan University
6-6 Asahigaoka, Hino, Tokyo 191-0065, JAPAN
nakano@aero.sd.tmu.ac.jp

Masahito ASAI
Department of Aerospace Engineering
Tokyo Metropolitan University
6-6 Asahigaoka, Hino, Tokyo 191-0065, JAPAN
masai@sd.tmu.ac.jp

ABSTRACT

Development of wake vortices and the associated sound radiation from a rectangular cylinder with various aspect ratios AR is studied by direct numerical simulations at Reynolds number 150 and Mach number 0.3. Both the lift and drag fluctuations operate as dipole sources from which acoustic waves are radiated in the lift and drag directions, respectively. The lift-dipole becomes the strongest at AR=0.5 where the Strouhal number of vortex shedding takes a maximum. On the other hand, the magnitude of drag dipole becomes pronounced for $AR \leq 1$ and increases with decreasing AR. The sound generated by the drag dipole is observed only in the upstream region. It is also found that for the smaller aspect ratios less than AR=0.5, the primary wake vortices soom alignes in two row, which forms the absolutely unstable region in the dounstream region, leading to formation of secondary vortex street far downstream.

INTRODUCTION

When a bluff body is placed in the uniform flow, the von Kármán vortex shedding occured for a wide range of Reynolds numbes, which induces the unsteady aerodynamic forces to the body. In addition, vortex induced pressure fluctuations form a dipole sound source on the body surface, dominating acoustic far field when the Mach number of uniform flow is low.

The self-sustained wake oscillations leading to the formation of Kármán vortex street is due to the development of global instability mode (Huerre & Monkewitz 1990, Chomaz 2005). Most of studies related to the bluff body wake have been done for circular-cylinder wake, where self-sustained wake oscillation occurs at Reynolds number above 46, and the Kármán vortex street becomes three dimensional and undergoes transition to turbulence downstream at Reynolds number above 200 (Williamson 1996). For Reynolds number less than Re=200, the primary Kármán vortex street decays and a stationary wake flow (laminar flow) develops (Cimbara et al. 1988). Then a secondary larger scale vortex street can appear further downstream (typically distance of more than 100 times the cylinder diameter); see Taneda (1959), Okude (1980), Karasudani & Funakoshi (1994), Inoue & Yamazaki (1999).

For wake of square cylinder, transition process is almost the same as that of circular-cylinder wake (Sohankar et al. 1999, Luo et al. 2003) though due to the flow separation at the upstream corners of cylinder, the Strouhal number is smaller than that in the cylindar wake, i.e. St=0.16 at Re>200 for square cylinder. As for the wake of rectangular cylinder of our interest, the wake structure and associated aerodynamic forces are known to strongly depend on aspect (width-to-height) ratio of cylincer cross-section. Nakaguchi et al. (1968) experimantally studied Strouhal number and drag force for rectangular cylinder with various aspect ratios upto AR=4 at Reynolds number Re=2 - 6×10^4. They showed that drag became maximum at AR=0.6 while the Strouhal number was almost constant for AR<1. The Reynolds number dependency of the Strouhal number was examined in the wind tunnel and

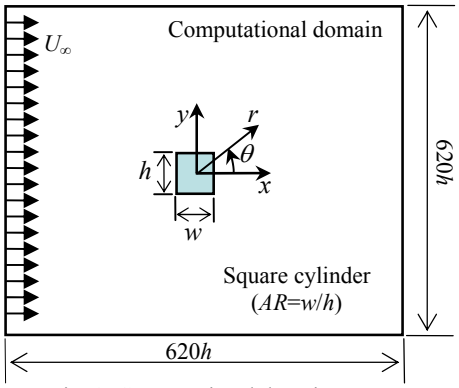

Fig. 1. Computational domain.

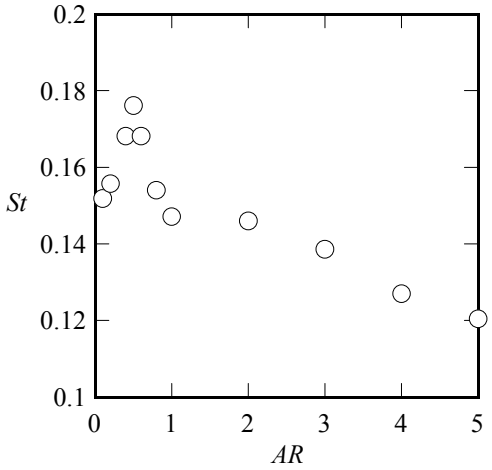

Fig.2. Strouhal number vs. aspect ratio *AR*.

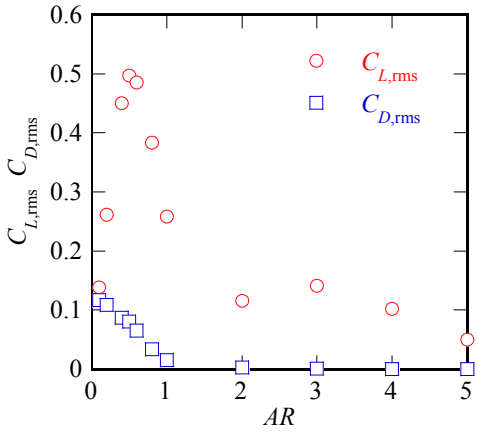

Fig. 3. The r.m.s. value of lift and drag fluctuations vs. aspectratio *AR*.

water tunnel experiment by Okajima (1982) for rectangular cylinders with *AR*=1, 2, 3 and 4 at Reynolds number ranged from *Re*=70 to 2×10^4. He reported that the Strouhal number was decreased suddenly for the rectangular cylinders with *AR*=2 and 3 at Reynolds numbers of 600 and 1000, respectively, though the value remained almost constant for the cylinder with *AR*=1 and 4. Numerical study by Davis and Moore (1982) demonstrated that both Strouhal number and magnitude of lift and drag fluctuations for rectangular cylinder with *AR*=0.6 became larger than those for *AR*=1 at Reynolds number *Re*=250. Sakamoto et al. (1989) experimentally studied aerodynamic forces of rectangular cylinder with aspect ratios between *AR*=0.3 and 2.5 at Reynolds number *Re* = 5.5×10^4 and showed that magnitude of both lift and drag fluctuations changed drastically for smaller aspect ratio cylinder less than *AR* = 1 and became the maximum at *AR*=0.7.

It is also expected that sound radiation from the rectangular cylinder highly depends on the aspect ratio of the cross section. However, vortex shedding and associated sound radiation in the bluff-body wake are examined only for ciurular and square cylinders (Inoue & Hatakeyama 2002, Inoue et al. 2006, Fujita 2010). In the present study, in order to understand how critically the development of wake vortices due to global instability and the associated sound generation depend on the aspect ratio, the flow around the rectangular cylinder with various aspect ratios between *AR*=0.1 and *AR*=5 are examined by direct numerical simulations of the compressible Navier-Stokes equations.

NUMERICAL SCHEME

We considered a two-dimensional flow past a cylinder with rectangular cross section, as illustrated in Fig. 1. The compressible Navier-Stokes equations were solved numerically by using the finite difference method with 6th order (4th order near the boundary) compact Padè scheme. The time advancement was implemented by the 4th order Runge-Kutta method. To avoid unphysical large wave-number oscillations, 8th order (6th order near the boundary) compact filter was applied at each time step. The uniform flow was given as an initial condition. The Navier-Stokes characteristic boundary condition (NSCBC) (Poinsot & Lele 1992) was used on the cylinder surface as well as outer (inflow and outflow) boundaries. The adiabatic non-slip condition was applied on the cylinder surface. In the present study, Cartesian (x, y) coordinate as well as polar (r,θ) coordinate is used, where the origin is located at center of the cylinder cross-section. In the computation, the coordinate is non-dimensionalized by height of cylinder h, and other physical quantities are normalized by those of the oncoming uniform flow.

Non-uniform rectangular grid of 1001×1001 grid points was used. The grid spacings are $\Delta x=\Delta y=0.025$ ($0<|x|<3$, $0<|y|<3$), $\Delta x=\Delta y=0.4$ ($10<|x|<100$, $10<|y|<100$) and $\Delta x=\Delta y=10$ ($120<|x|<620$, $120<|y|<620$), and these regions are connected smoothly. The Reynolds number based on the uniform flow velocity and the height of rectangular cylinder was fixed at 150 and the Mach number at the inflow boundary was 0.3.

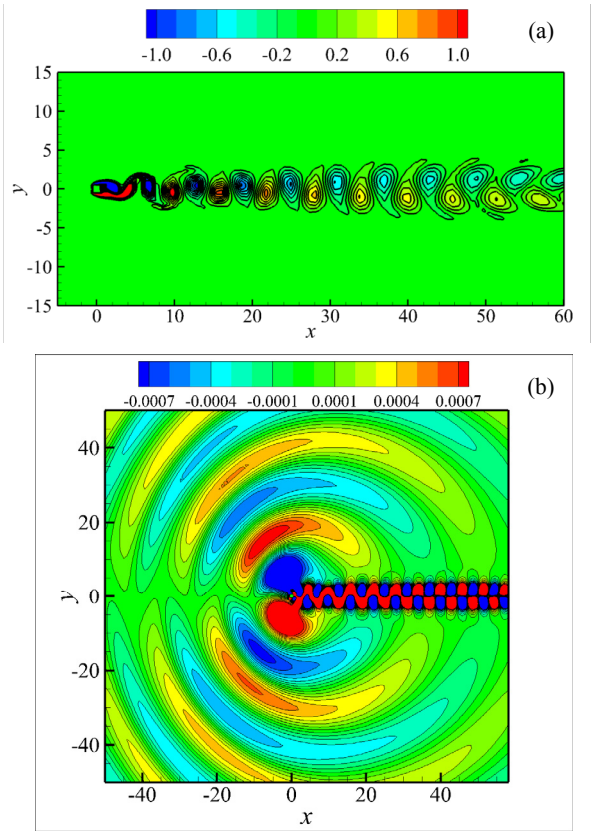

Fig. 4. Contour maps of (a) vorticity and (b) pressure fluctuation for the square cylinder (AR=1, M=0.3, Re=150).

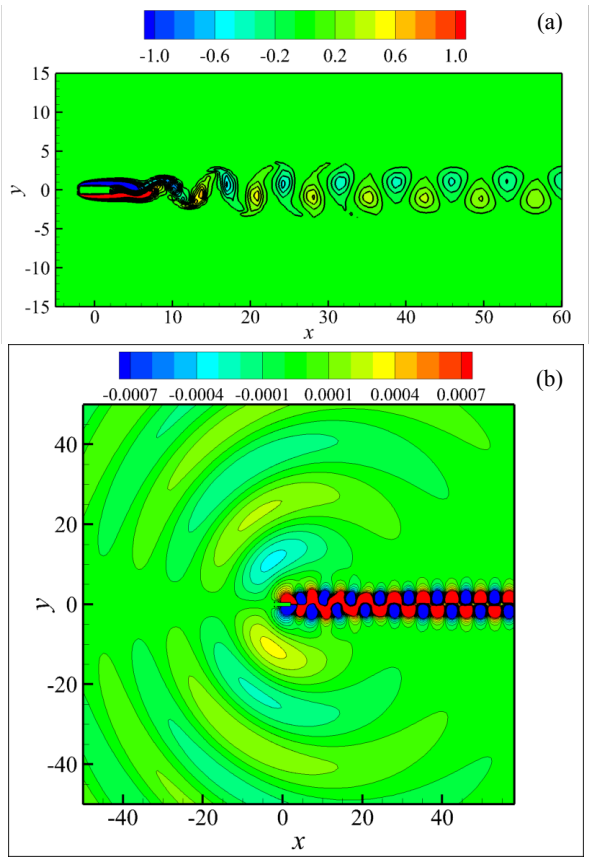

Fig. 5. Contour maps of (a) vorticity and (b) pressure fluctuation for AR=4..

RESULTS AND DISCUSSION

Figure 2 illustrates dependency of the aspect ratio on the Strouhal number of primary von Kármán vortex street, showing that the Strouhal number monotonically decreases as AR increases for AR>1 though the value drastically varies at AR<1, where the Strouhal number takes a maximum at AR=0.5. The magnitudes of lift and drag fluctuations are plotted against the aspect ratio AR in Fig. 3. Similar to the Strouhal number variation, the magnitude of lift fluctuation becomes a maximum at AR=0.5. On the other hand, the magnitude of drag fluctuation monotonically decreases with increasing AR.

Wake vortices and associated sound ratiation are examined in deail for the three different cases of AR=0.4, 1 and 4. Figures 4(a) and 4(b) illustrate contour maps of vorticity and pressure fluctuation, respectively, in the case for square cylinder (AR=1). We see von Kármán vortex street in the wake of the cylinder, where vortex formation occurs at and around x=5 (Fig. 4a). The Strouhal number is St=0.147, which is very close to that of the past numerical study for square-cylinder wake at Re=150 at M=0.2 by Inoue et al. (2006). Sound radiation occurs at the frequency of Kármán vortex shedding (f=F_K) in the transverse direction, in Fig. 4(b), indicating that sound by the lift dipole dominates the acoustic far field. Note that owing to the doppler effect, directivity of the sound wave is the strongest not at θ=90deg but at θ=110deg for present M=0.3 condition. The radiated sound is weakened with increasing the aspect ratio as shown in Fig. 5(b), where the vortex formation occurs at x≈10, slightly downstream compared with the case for AR=1 (Fig. 5a). In this case, the flow separated at the upstream corners is reattached and the boundary layer develops on the cylinder surface, which makes the wake shear layer thicker, and the magnitude of reversed flow downstream of trailing edge is smaller, weakening the absolutely unstable nature in the wake.

For the smaller aspect ratio of AR=0.4, on the other hand, the vortex formation occured immediately downstream of the cylinder as in Fig. 6(a). Interestingly, the wake vortices soon align in two rows along y=±2 at 12≤x≤40, and we can see development of a secondary vortex street whose wavelength is much larger than that of the primary vortices in the downstream locations for x>40. The friquency of secondary secondary vortex formation is not a subharmonic of that of the primary vortex shedding, indicating that the secondary

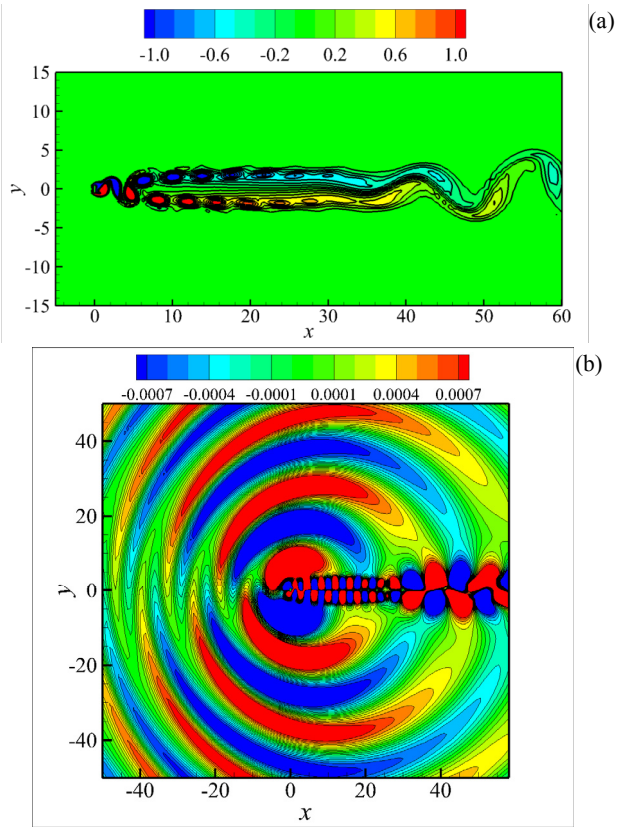

Fig. 6. Contour mape of the pressure fluctuation for (a) AR=1 and (b) AR=0.4.

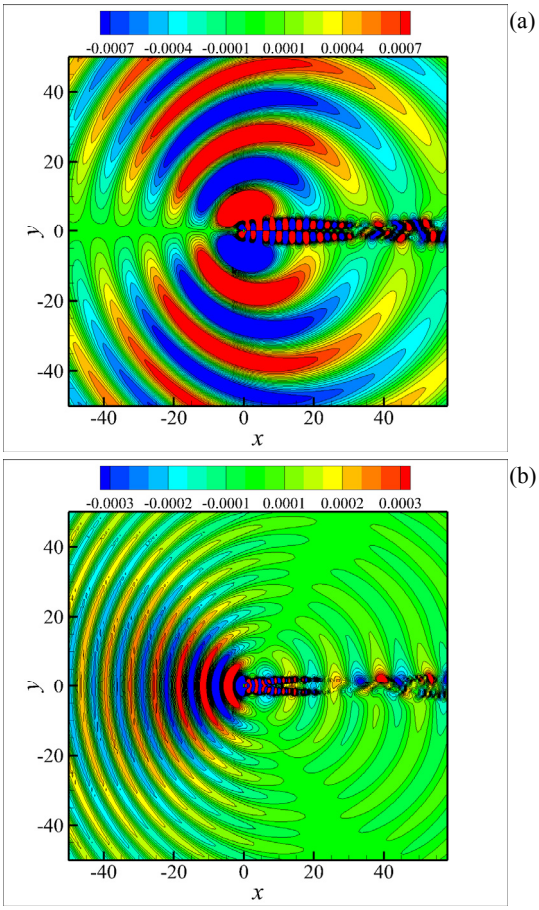

Fig. 7. Contour map of instantaneous sound pressure for AR=0.4. Frequency components of $f=F_K$ and $f=2F_K$ are singled out in (a) and (b), respectively.

vortices are created not by the pairing of the primary vortices but by the instability of flow. The instability mechanism leading to the secondary vortex street will be discussed later. The sound radiation related to the secondary vortex formation is haldly observed at present low Mach number condition. It should be noted that the formation of the secondary vortices was found only for $AR \leq 0.5$ at this Reynolds number. The sound intensity, Fig. 6(b), is considerably larger than the case for AR=1 due to closer formation of wake vortices, and sound wave propagates not only to the transver direction but also to the streamwise (upstream) direction, implying that the sound by the drag dipole whose frequency is $2F_K$, twice the frequency of Kármán vortex shedding, becomes significant there. To assure this, the acoustic fields by the lift and drag dipoles are examined in more detail by FFT and the resuls are demonstrated in Figs. 7(a) and 7(b) which display acoustic fields of the frequency $f=F_K$ and $2F_K$, respectively. The sound with $f=2F_K$ is generated by drag fluctuations and mainly propagates in the upstream direction (Fig. 7b), which is on the contrary to the prediction from Curl's acoustic analogy while the acoustic field with $f=F_K$ is almost the same as that for AR=1 except its intensity (Fig. 7a).

The dependency of intensity of sound by the lift and drag dipoles on the aspect ratio AR is plotted in Fig. 8. Here, maximum rms value of sound wave at r=75 is plotted. Corresponding to the variations of magnitude of lift fluctuations as shown in Fig. 2, the sound level by the lift dipole becomes maximum at AR=0.5. Figure 9 demonstrates rms valus of pressure fluctuation on the cylinder upper-surface for three different aspect ratios of AR=0.2, 0.5 and 1. In comparison with AR=1, the magnitude of pressure fluctuation becomes large due to closer formation of vortices for both AR=0.5 and 0.2 cases while the difference between AR=0.2 and 0.5 cases is small, indicating that the location of vortex formation already reaches the upstream limit (immediately downstream the cylinder) at AR=0.5. Besides, decrease in upper and lower surface area of cylinder results in attenuation of the sound by the lift dipole for AR<0.5. Drag-dipole generating sound level increases with decreasing AR, and becomes almost same as that by th the lift dipole for the smallest aspect ratio of AR=0.1. Thus, the sound by the drag diple becomes significant relatively to the lift-dipole sound for smaller aspect ratio less than AR=0.1.

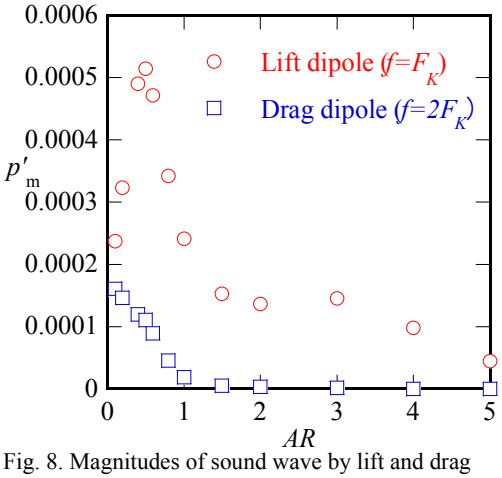

Fig. 8. Magnitudes of sound wave by lift and drag dipoles at r=75 vs. aspect ratio.

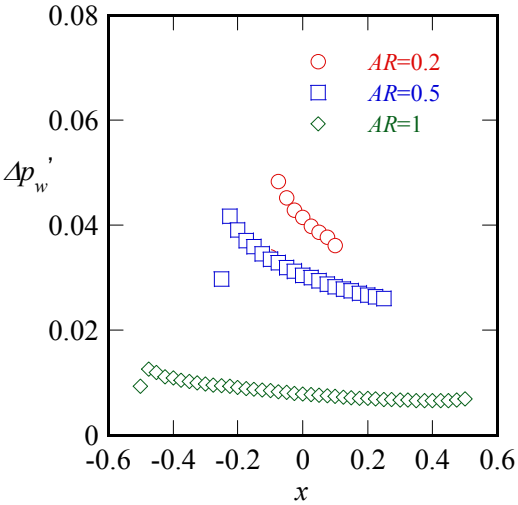

Fig. 9. r.m.s. value of pressure fluctuation on the cylinder upper-surface for various aspect ratio.

Finally, we examine the instability mechanism leading to secondary vortex street. Figure 10 illustrates contour map of the mean streamwise velocity U in the case for AR=0.4. We see low velocity region ($U < 0.1$) around the center line (y=0) at $10 \le x \le 40$, and the minimum velocity at y=0 is found to be about U=0.03 at and around $x \approx 20$. According to the linear stability analysis with paralle flow assumption by Monkewitz (1988), the absolutely unstable nature arises in the wake velocity profile when the center line velocity is less than 5% of the uniform flow velocity. Therefore, absolute instability mechanism may govern the secondary vortex formation. To confirm this, linear stability analysis on the basis of incompressible Rayleigh stability equation was carried out. The mean velocity profile at x=20 was approximated by using 3rd order spline function as displayed in Fig. 11(a). Figure

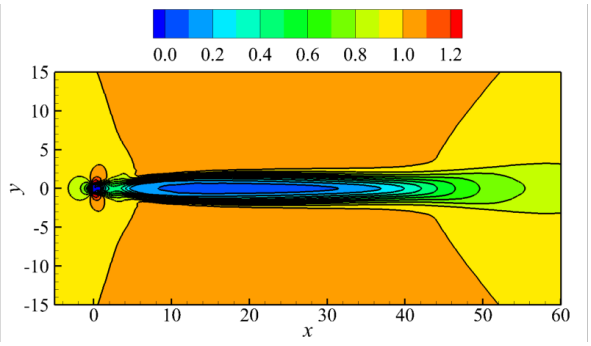

Fig. 10. Contour map of mean streamwise velocity U in the wake of rectangular cylinder with AR=0.4.

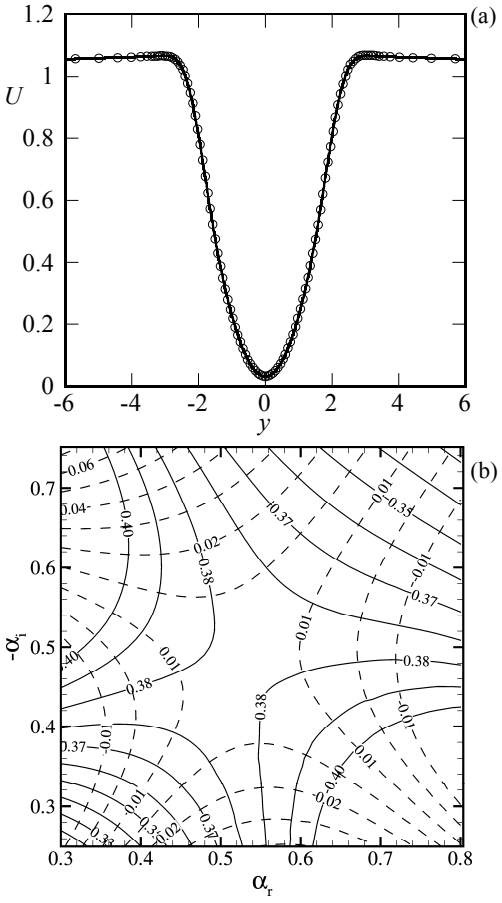

Fig. 11. (a) The mean celocity profile and (b) eigenvalue ω of the linear stability equation on complex α-plane at x=20 for AR=0.4. A solid curve in (a) represents approximation by the spline function. In (b), solid and broken lines are ω_r and ω_i, respectively.

11(b) illustrates the eigenvalues in the complex wavenumber plane, showing that the temporal growth rate at the saddle

point, where the group velocity $c_g=d\omega/d\alpha$ is 0, is positive ($\omega_{i,s}$=0.095) and thus the flow is absolutely unstable at x=20. The angular frequency at the saddle point is $\omega_{r,s}$ = 0.384 which coincides with the DNS result (0.380). Thus, the vortex streets in the wake of rectangular cylinder with small aspect ratio is dominated by the two different alsolute (global) instability modes.

CONCLUSIONS

Development of wake vortices and the associated sound radiation were studied for the wake of a rectangular cylinder with various aspect ratios *AR* by direct numerical simulations at the Reynolds number 150 and Mach number 0.3.

In the case of square cylinder of *AR*=1, the sound by the lift dipole whose frequency is the same as that of von Kármán vortex shedding donimated the acoustic far field. With increasing the aspect ratio above *AR*=1, the location of vortex formation shifted downstream location and the intensity of the radiated sound became weak. With decreasing the aspect ratio below *AR*=1, on the other hand, the lift-dipole became stronger and took the maximum value at *AR*=0.5 where the Strouhal number of vortex shedding was also a maximum. Due to decrease in the area of upper and lower surfaces, the intensity of the lift dipole was rapidly weakened as the aspect ratio decreased for *AR*<0.5. Contribution of drag-dipole to the acoustic far field became stronger with decreasing *AR* for *AR* ≤ 1. The sound generated by the drag dipole was observed only in the upstream region. It is also found that for the smaller aspect ratios less than *AR*=0.5, the primary wake vortices soom aligned in two row, which formed the absolutely unstable region leading to secondary vortex street downstream without prominent sound ratiation.

REFERENCES

Chomaz, J.M., 2005, "Global instabilities in spatially developing flows: non-normality and nonlinearity" *Annu. Rev. Fluid Mech.*, 37, pp. 357-392.

Cimbala, J. M., Nagib, H. M. and Roshko, A., 1988, "Large structure in the far wakes of two-dimensional bluff bodies", *J. Fluid Mech.*, 190, pp. 265-298.

Davis, R. W. and Moore, E. F., 1982, "A numerical study of vortex shedding from rectangles", *J. Fluid Mech.*, 116, pp. 475-506.

Fujita, H., 2010,"The characteristics of the Aeolian tone radiated from two-dimensional cylinders", *Fluid Dyn. Res.*, 42, pp. 1-25.

Huerre, P. and Monkewitz, P.A., 1990, "Local and global instabilities in spatially developing flows", *Annu. Rev. Fluid Mech.* 22, pp. 473-537.

Inoue, O. and Hatakeyama, N., 2002, "Sound generation by a two-dimensional circular cylinder in a uniform flow", *J. Fluid Mech.*, 471, pp. 285-314.

Inoue, O., Mori, M. and Hatakeyama, N., 2006, "Aeolian tones radiated from flow past two square cylinders in tandem", *Phys. Fluids*, 18, 046101.

Inoue, O. and Yamazaki, T., 1999, "Secondary vortex streets in two-dimensional cylinder wakes", *Fluid Dyn. Res.*, 25, pp. 1-18.

Karasudani, T. and Funakoshi M., 1994, "Evolution of a vortex street in the far wake of a cylinder", *Fluid Dyn. Res.*, 14, pp. 331-352.

Luo, S. C., Chew Y. T. and Ng Y. T., 2003, "Characteristics of square cylinder wake transition flows", *Phys. Fluids*, 15 (9), pp. 2549-2559.

Monkewitz, P. A., 1988, "The absolute and convective nature of instability in two-dimensional wakes at low Reynolds numbers", Phys. Fluids, 31 (5), pp. 999-1006.

Nakaguchi, H., Hashimoto, K. and Muto, S., 1968, "An experimental study of aerodynamic drag of rectangular cylinders", *J. Japan Soc. Aero. Apace Sci.*, 16, pp. 1-5.

Okajima A., 1982, "Strouhal numbers of rectangular cylinders", *J. Fluid Mech.*, 123, pp. 379-398.

Okude, M., 1981, "Rearrangement of the Karman vortex street", *Trans. Japan Soc. Aero. Space Sci.*, 24, pp. 95-105.

Poinsot T. J. and Lele S. K., 1992, "Boundary conditions for direct simulations of compressible viscous flows", *J. Comp.Phys.*, 101, pp. 104-129.

Sakamoto, H., Haniu, H. and Kobayashi K, 1989, "Fluctuating forces acting on rectangular cylinders in uniform flow", *Trans. Japan Soc. Mech. Eng.*, 55-516, pp. 88-0135.

Sohankar A., Norberg C. and Davidson L., 1999, "Simulation of three-dimensional flow around a square cylinder at moderate Reynolds numbers", *Phys. Fluids*, 11 (2), pp. 288-306.

Taneda, S., 1959,"Downstream development of the wakes behind cylinders" , *J. Phys. Soc. Japan*, 14, pp. 843-848.

Williamson C. H. K., 1996, "Vortex dynamics in the cylinder wake", *Annu. Rev. Fluid Mech.*, 28, pp. 477-539.